applied sciences

MDPI

Article

Resilience Evaluation of Shallow Circular Tunnels Subjected to Earthquakes Using Fragility Functions

Zhongkai Huang

Department of Geotechnical Engineering, Tongji University, Shanghai 200092, China; 5huangzhongkai@tongji.edu.cn

Abstract: The present work aims to introduce an integrated framework for the resilience evaluation of shallow circular tunnels subjected to earthquakes using fragility and restoration functions. A typical shallow circular tunnel in Shanghai city of China is examined in this work and a corresponding numerical model is established using ABAQUS. Then, a set of ground motions are well chosen to implement large numbers of non-linear numerical analyses so as to determine the lining responses of the tunnel structure with various levels of seismic intensities. According to the above numerical results, fragility functions in terms of the peak ground acceleration (*PGA*) and peak ground velocity (*PGV*) at the free-field ground surface are generated, accounting for the main sources of uncertainty, and the direct seismic loss for the examined tunnel is obtained. Moreover, according to the developed fragility functions and the existing empirical tunnel restoration functions, the evolution of the resilience index (*Re*) with various levels of *PGA* and *PGV* for the examined tunnel is derived and quantified. The results indicate that the tunnel resilience will decrease significantly as the earthquake intensity measure (*IM*), i.e., *PGA* or *PGV* herein, increases. The proposed framework is expected to help city managers support adaptations to seismic hazards with the development of preventive or retrofitting measures as part of efforts to provide more resilient metro systems.

Keywords: seismic resilience; circular tunnel; fragility function; loss assessment

Citation: Huang, Z. Resilience Evaluation of Shallow Circular Tunnels Subjected to Earthquakes Using Fragility Functions. *Appl. Sci.* **2022**, *12*, 4728. https://doi.org/10.3390/app12094728

Academic Editors: Rui Wang, Jian-Min Zhang and Lanmin Wang

Received: 23 April 2022
Accepted: 7 May 2022
Published: 8 May 2022

1. Introduction

In recent decades, the increasing intensity and frequency of earthquakes have posed a significant risk to operational tunnels [1]. For instance, in China, after the 2008 Wenchuan earthquake, numerous tunnels were reported to have suffered from different degrees of damage [2], causing significant economic losses and casualties. Moreover, tunnels constitute crucial elements of transportation infrastructure worldwide; seismically induced damage of tunnels may thus have substantial consequences on the operation of the global transportation network after a significant event [3]. Therefore, a thorough study of the resilience evaluation of tunnels is of paramount importance to the development of better seismic infrastructure planning and interventions.

Seismic resilience describes the capability of a tunnel and associated organizations and communities to mitigate damage induced by earthquake loading [4], these factors constituting the key components in vulnerability and risk analyses for metro systems. Tunnels that are resilient to earthquakes can maintain and even enhance their crucial functionality by responding and adjusting to seismic events. In this sense, resilience can be associated with organizational, technical, social, and economic dimensions [5]. Critical infrastructure assessments based on the concept of resilience have been at the forefront of research for decades [6,7] and are gradually being integrated into the design practices and operational procedures of transport infrastructure stakeholders [8,9].

Quantifying infrastructure resilience is typically associated with the so-called resilience indexes, which describe the assets' ability to absorb the effects of damage, adjust to new circumstances, and return to normal after failure [9,10]. Moreover, indexes related to

the resilience curve, which describes how well a structure recovers after an earthquake event and how quickly it can return to full functionality, are widely used [8–10]. The resilience assessment frameworks for single and multiple hazards have been developed and applied to a variety of infrastructures, such as hospital facilities [11,12], schools [13,14], transportation networks [9,10], buildings [15,16] and bridges [17,18]. These existing works have been conducted with various assumptions and have some limitations [19–21]; thus, there is a need for further studies related to the development of more rigorous resilience assessment frameworks for different types of infrastructure. Additionally, there have been recent introductions of resilience considerations for tunnels that account for the effects of extreme surcharge discussed by Huang and Zhang [22]; nevertheless, to the author's best knowledge, such an evaluation framework related to the seismic resilience of tunnels has not been considered in the literature.

To bridge this gap, this study extends the author's previous investigation published at the 4th International Conference on Performance-Based Design in Earthquake Geotechnical Engineering (PBD-IV) [23] to further shed light on the resilience of shallow circular tunnels subjected to earthquakes using fragility functions. This study focuses on the probabilistic seismic resilience evaluation of circular tunnels in typical soft soil areas. The seismic resilience of the examined tunnel is quantified based on the developed fragility functions and existing restoration functions. The effects of various fragility functions proposed by different researchers on tunnels' resilience are also highlighted. The findings of this study are expected to assist consultants, operators, and stakeholders in enhancing seismic risk management as part of the development of more resilient metro systems.

2. Seismic Resilience Evaluation Framework

Seismic resilience is a helpful measure for investigating a tunnel's ability to withstand various levels of earthquake intensity. In this study, tunnel resilience is assessed by utilizing the following steps, as shown in Figure 1. First, the examined tunnel properties and soil site information are introduced (step (a)). Then, ground motions are well-chosen to cover sufficient variabilities (step (b)). Based on this, a numerical model is developed for the selected soil–tunnel system by ABAQUS, and large numbers of dynamic analyses are conducted (step (c)). Afterwards, the relationship between the examined tunnel's damage index (*DI*) and selected intensity measure (*IM*) is determined (step (d)). Following this step, the corresponding fragility functions are proposed in terms of selected *IM*s (step (e)). Finally, the loss function (step (f)) and seismic resilience curve (step (g)) are developed for the examined tunnel based on the above steps. The above seven steps are introduced in the following parts.

2.1. Modelling Soil–Tunnel Configurations

Steps (a), (b), and (c) in Figure 1 are introduced in detail in this section on Modelling Soil–Tunnel Configurations. A typical shield tunnel, located in Shanghai city of China, is used to perform a seismic resilience assessment, as shown in Figure 2. The circular tunnel is built in the soft soil profile, at a depth of 100 m, and lies on the elastic bedrock. This type of tunnel has a radius of 3.10 m, and a lining thickness of 0.35 m. Moreover, its elastic modulus (E_c) is 3.55 GPa, and its Poisson's ratio (v_c) is 0.2. As indicated in Figure 2, this tunnel has a buried depth (h) of 9.0 m; therefore, the tunnel overburden depth ratio (h/d) is equal to 1.45. This is a typical case of a shallow tunnel.

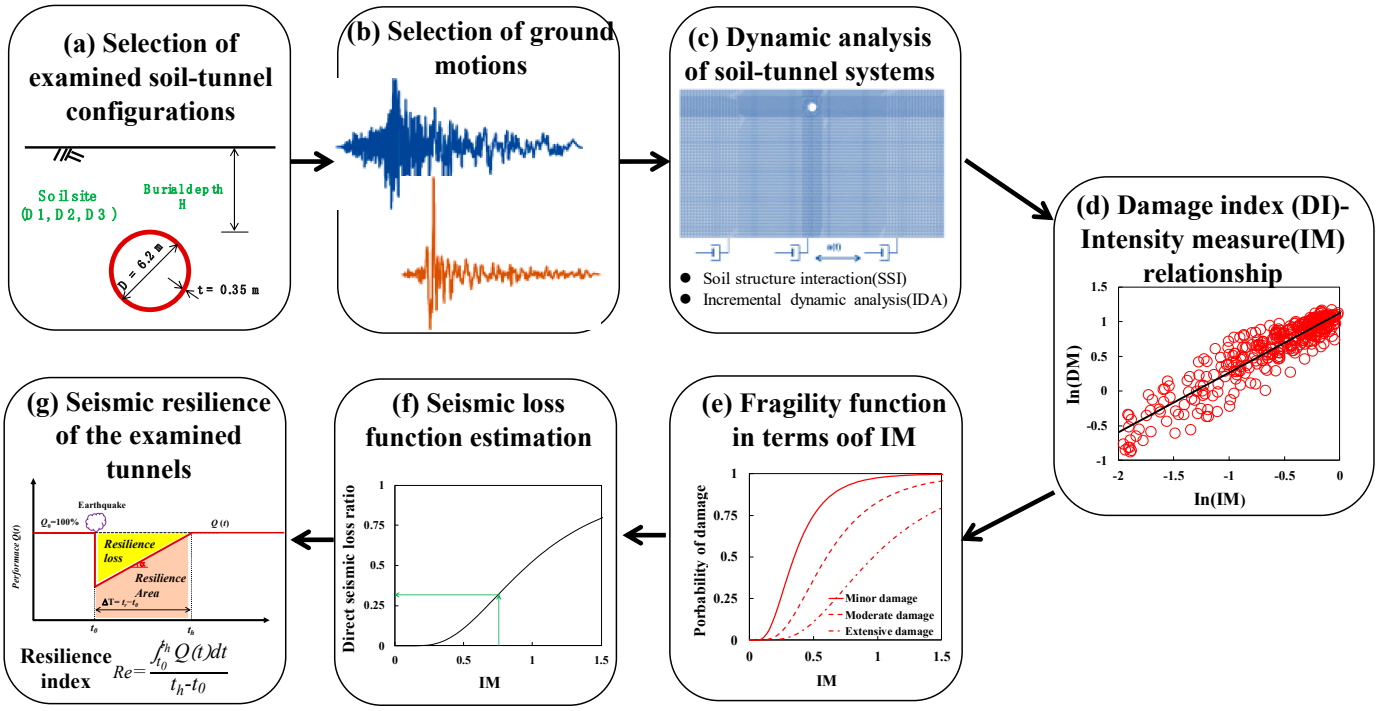

Figure 1. Proposed framework to evaluate the seismic resilience of tunnels.

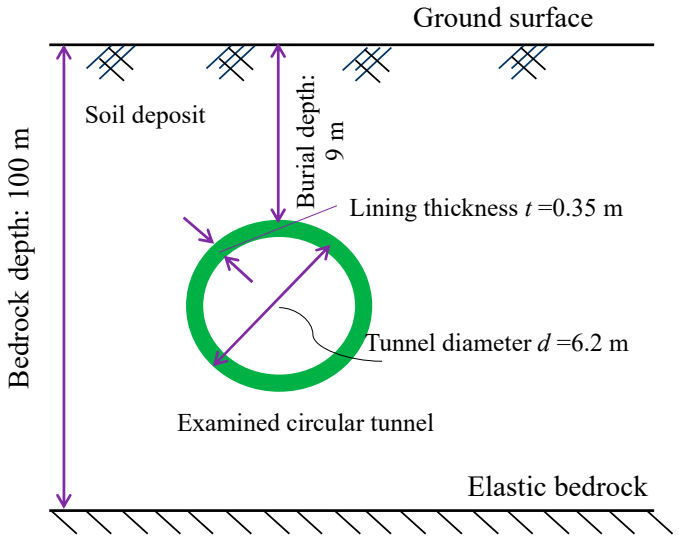

Figure 2. Diagrammatic sketch for the examined circular tunnel (not to scale).

Three soil profiles are chosen and classified as soil type D according to EC8 [24]; they are further referred to as soil deposits D1, D2, and D3 in this work. For all three selected soil profiles, the detailed developments of shear wave velocities (V_s), density (ρ), cohesion (c), and friction angle (φ) along the soil height are presented in Figure 3, respectively. Additionally, Figure 4a,b show the typical G-γ-D curves for clayey and sandy layers, respectively. The author's previous work could be used to check more details about the selected soil profiles [23].

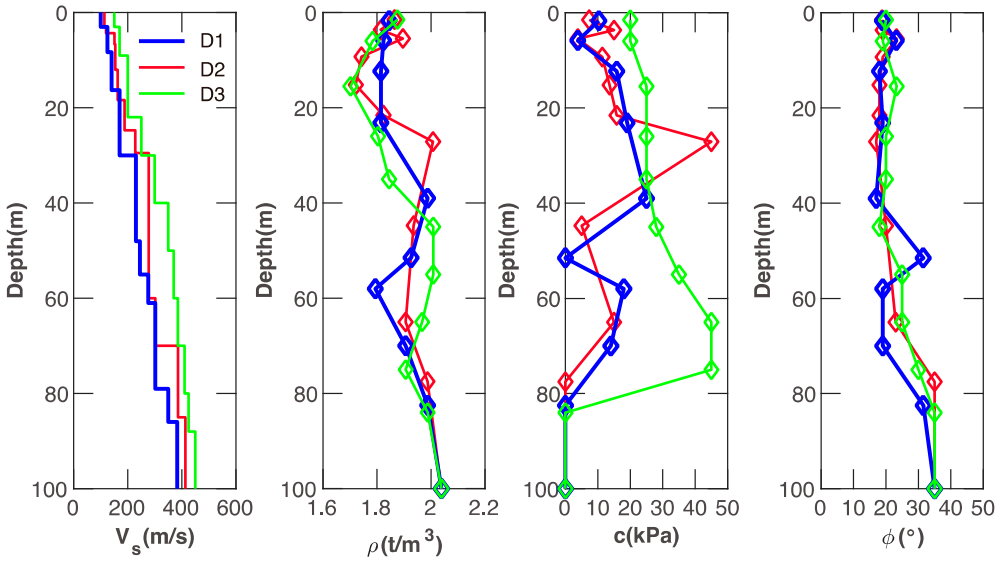

Figure 3. Geotechnical parameters of the examined soil profiles.

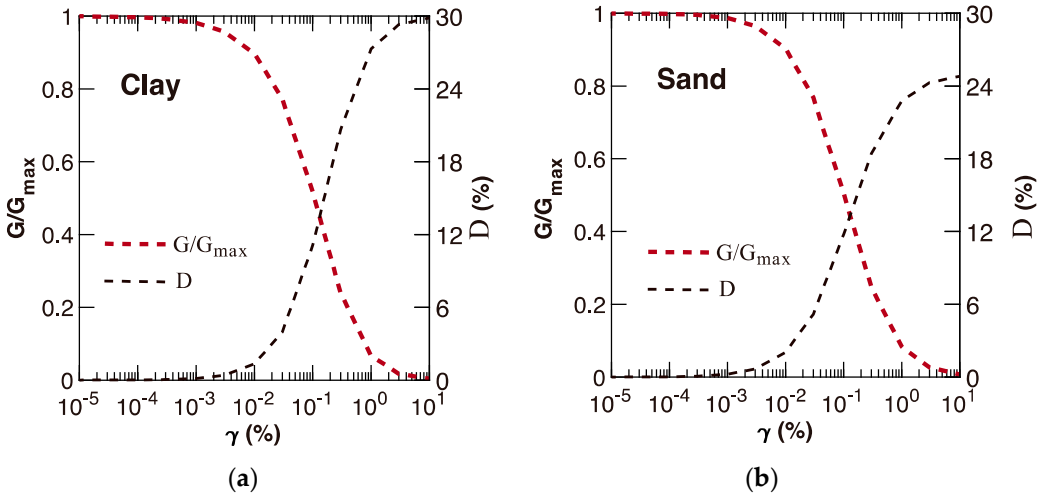

Figure 4. *G*-γ-*D* curves for (**a**) clayey layers and (**b**) sandy layers [23].

Figure 5 shows a detailed two-dimensional (2D) finite element model of the studied soil–tunnel configuration generated by the platform ABAQUS. This model has a height of 100 m and a width of 400 m. As for the base boundary of the model, it is simulated as an 'elastic bedrock' using the method of Lysmer and Kuhlemeyer [25] by setting appropriate dashpots, where the selected ground motions are inputted. For the lateral boundaries of the model, a kinematic tie constraint is set to let the opposite vertical sides move at the same time. The tunnel–soil interface is appropriately simulated by a finite sliding hard contact algorithm provided by ABAQUS. The tangential behavior is reflected based on the penalty friction formulation by introducing a commonly used Coulomb frictional model with a friction parameter (μ) equal to 0.6. The response of tunnel lining is modeled by a simple linear elastic model. A uniform tunnel lining is adopted in the numerical model, focusing the computational efficiency in the analyzed cases. A Mohr–Coulomb model is utilized to capture the non-linear behavior of soil in the dynamic analysis. Each analysis is performed in two consequent steps, i.e., a geostatic step followed by a dynamic analysis step. The first step is conducted to build the geostatic stress equilibrium within the numerical model. In contrast, the acceleration time history is introduced via dashpots at the model's base in the second step. More details about the numerical model development could be checked in the author's previous work [23].

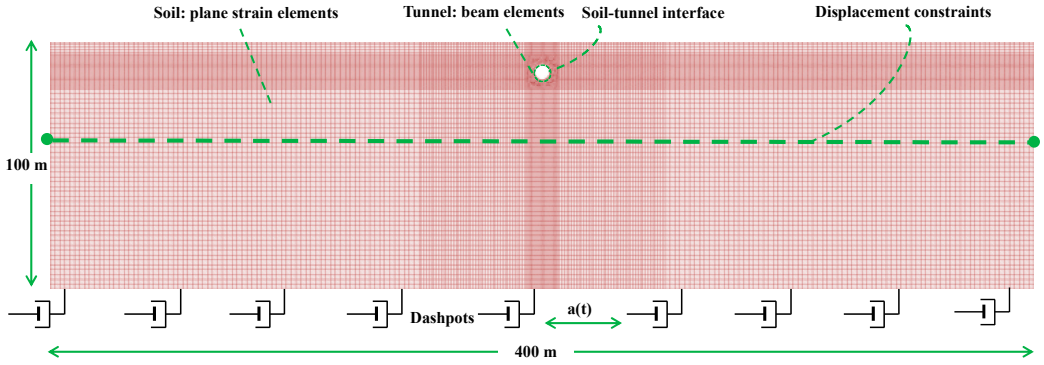

Figure 5. Soil–tunnel interaction model.

It is very important to choose a set of ground motions that cover a high level of uncertainty within the seismic fragility analysis of any element at risk so as to perform an accurate seismic risk assessment. Table 1 shows the general properties of the selected 12 seismic ground motions in this work, which are provided by the Pacific Earthquake Engineering Research Strong Motion Database (https://ngawest2.berkeley.edu accessed on 10 April 2020). These ground motions are scaled from 0.1 g to 1.0 g, with a gradient of 0.1 g, and then applied in the numerical modeling. More information about the selection of the adopted seismic records can be found in the author's work for the PBD-IV [23].

Table 1. Selected ground motions [23].

No.	Earthquake	Station Name	Year	Mag. (M_w)	R_k (km)	*PGA* (g)
1	Northridge-01	LA-Hollywood Stor FF	1994	6.69	19.73	0.23
2	Parkfield	Cholame-Shandon Array	1966	6.19	12.9	0.24
3	Loma Prieta	Treasure Island	1989	6.93	77.32	0.16
4	Kern County	Taft Lincoln School	1952	7.36	38.42	0.15
5	San Fernando	Castaic-Old Ridge Route	1971	6.61	19.33	0.34
6	Imperial Valley-02	El Centro Array #9	1940	6.95	6.09	0.28
7	Superstition Hills-01	Imperial Valley W.L. Array	1987	6.22	17.59	0.13
8	Parkfield-02_CA	Parkfield-Cholame 2WA	2004	6.00	1.63	0.62
9	Imperial Valley-07	El Centro Array #11	1979	5.01	13.61	0.19
10	Tottori_Japan	TTR008	2000	6.61	6.86	0.39
11	Kobe_Japan	Port Island	1995	6.9	3.31	0.32
12	Borrego Mtn	El Centro Array #9	1968	6.63	45.12	0.16

2.2. Generation of Fragility Functions

As illustrated in Equation (1), most fragility functions could be expressed using a cumulative lognormal probability distribution function [15–17]:

$$P(ds \geq ds_j \Big| IM) = \Phi\left[\frac{1}{\beta_{tot}} \cdot \ln\left(\frac{IM}{IM_{mj}}\right)\right], \quad (1)$$

where $P(ds \geq ds_j \mid IM)$ represents the exceedance probability of a specific damage state, i.e., *DS* or *ds*, under an earthquake intensity level, the latter being described through the earthquake intensity measure *IM*, i.e., *PGA* or *PGV* in this work; $\Phi(\bullet)$ represents the cumulative distribution function; IM_{mj} stands for the mean value of *IM* needed to induce the j_{th} *ds*; and β_{tot} stands for the total standard deviation, which can be calculated through the combination of three main sources of uncertainty, as illustrated in Equation (2):

$$\beta_{tot} = \sqrt{\beta_{ds}^2 + \beta_C^2 + \beta_D^2}, \quad (2)$$

where β_{ds} is the uncertainty involved in defining various damage states; β_C is used to quantify the uncertainty associated with the response of the structure (seismic capacity); and β_D is utilized to describe the uncertainty originating from the ground motions (seismic demand). The parameters of β_{ds} and β_C are assumed to be 0.4 and 0.3, respectively [26].

A damage index (*DI*) is utilized to appropriately characterize various damage states and is defined using the ratio of the actual (M) over the capacity (M_{Rd}) bending moment of the tunnel lining cross-section [26]. On this basis, the capacity (M_{Rd}) bending moment of the tunnel lining is assessed by a section analysis [26] according to the material and geometric characteristics of the lining, taking into account the actual axial forces (N) and bending moments (M). Five damage states are introduced in Table 2.

Table 2. Information on damage states and corresponding damage indexes [26].

Damage State (*ds*)	Range of Damage Index (*DI*)	Central Value of *DI*
ds_0: none	$M_{sd}/M_{Rd} \leq 1.0$	-
ds_1: minor	$1.0 < M_{sd}/M_{Rd} \leq 1.5$	1.25
ds_2: moderate	$1.5 < M_{sd}/M_{Rd} \leq 2.5$	2.00
ds_3: extensive	$2.5 < M_{sd}/M_{Rd} \leq 3.5$	3.00
ds_4: complete	$M_{sd}/M_{Rd} \geq 3.5$	-

2.3. Direct Seismic Loss Analyisis

By using the above-proposed fragility functions, the probabilities of exceeding the particular damage states can be calculated. Subsequently, the direct seismic losses (S_{loss}s) of tunnels owing to structural damage after earthquake events can be evaluated using the following equation [27]:

$$S_{loss} = R_c \cdot L \cdot \sum_{j=1}^{n} \left(R_j \cdot P\left[DS_j | IM \right] \right), \tag{3}$$

where S_{loss} is the average estimated cost of repairing the tunnel, given the specific level of earthquake intensity measure, *IM*; R_c stands for the cost of tunnel replacement per meter; L is the length of the examined tunnels (L is set as 1 m in this study); the index j stands for the jth damage state (DS_j), and the index n represents the total number of damage states; R_j represents the repair ratio, which is the fraction of R_c necessary to repair the jth damage state; $P[DS_j \mid IM]$ represents the probability that the tunnel is located at each damage state j and seismic intensity level (*IM*), as presented in the following equations based on the fragility functions:

$$P\left[DS_j | IM \right] = P\left[ds > DS_{j+1} | IM \right] - P\left[ds > DS_j | IM \right], \text{ when } j = 1, 2, 3, \tag{4}$$

$$P\left[DS_j | IM \right] = P\left[ds > DS_j | IM \right], \text{when } j = 4. \tag{5}$$

More specifically, the replacement cost of the examined tunnel per meter (R_c) is assumed to be 1,000,000 RMB/m in this study, which is a preliminary estimate of the direct costs based on the construction cost of tunnels in China. The repair ratios (R_j) utilized in this work were put forward by Werner et al. [28] for tunnels, as shown in Table 3. For instance, a minor damage state of the tunnel indicates that the repair cost is equal to 10% of the total replacement cost. An example of using fragility functions under a specific seismic *IM* to calculate the direct seismic loss of tunnels is shown in Figure 6.

Table 3. Repair ratio of tunnels under different damage states [28].

Damage States (*DS*)	R_i, Repair Cost (% Replacement Cost)
No damage	0%
Minor damage	10%
Moderate damage	25%
Extensive to complete damage	75%

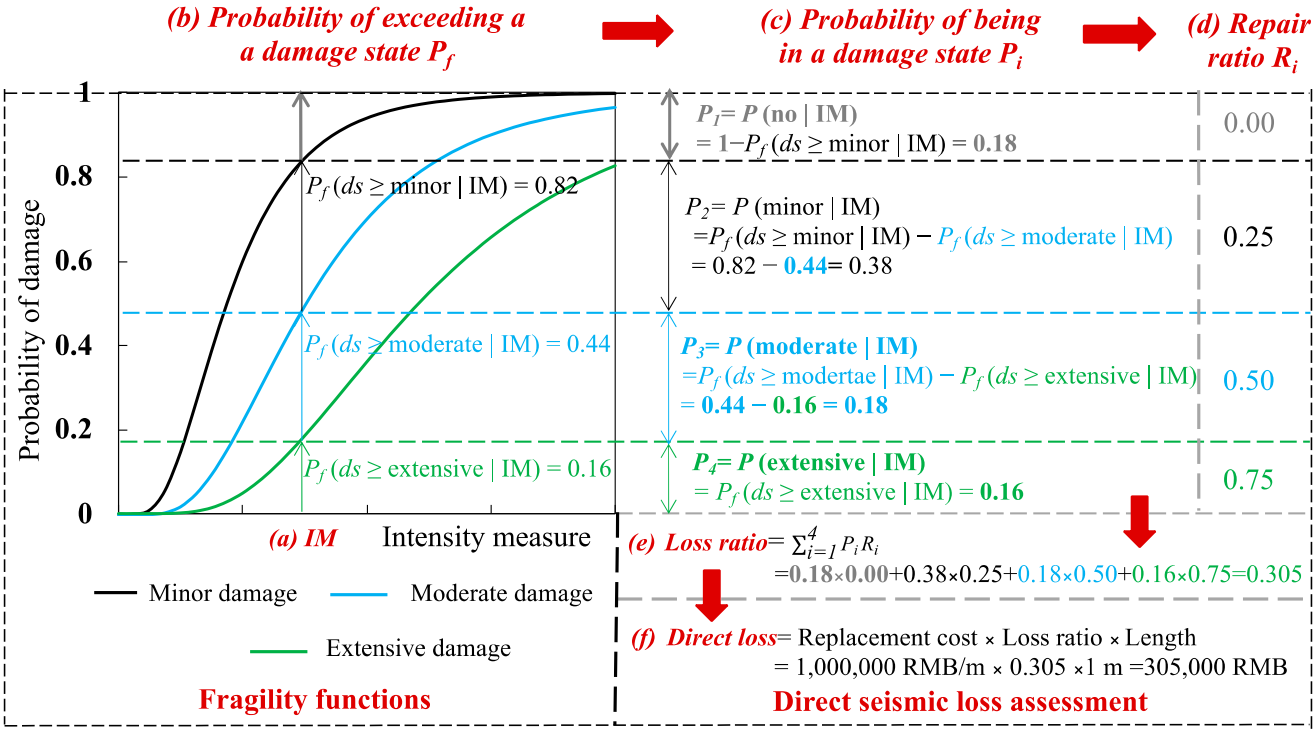

Figure 6. An illustrative case of using the fragility function for a given *IM* to calculate the direct seismic loss of tunnels.

2.4. Seismic Resilience Index Assessment Procedure

Resilience (*Re*) is a term used to describe the ability of tunnels to recover after being subjected to seismic damage. The most widely used analytical definition is adopted in this work. The following formula can be used to calculate *Re* [10,13]:

$$Re = \frac{\int_{t_0}^{t_h} Q(t)\mathrm{d}t}{t_h - t_0}, \tag{6}$$

where $Q(t)$ represents the tunnel functionality at time t under the functionality recovery function, t_0 is the earthquake occurrence time (t_0 is set as 0 in this study), and t_h is the investigated time point. As defined in Equation (3), the resilience index (*Re*) can be graphically illustrated, as shown in Figure 7.

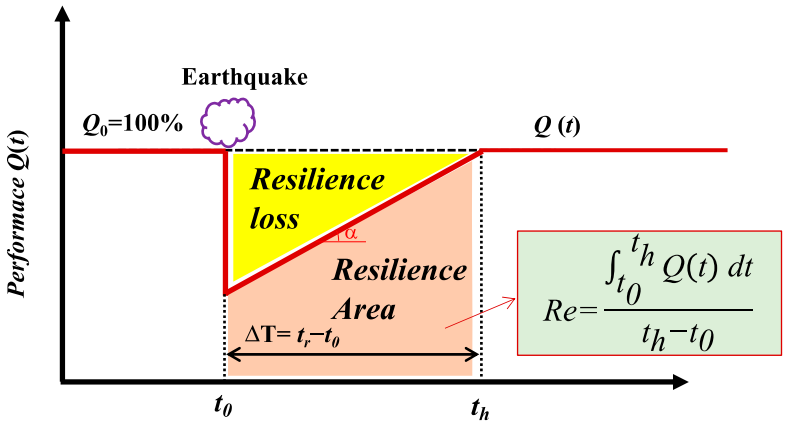

Figure 7. Definition of the resilience index (*Re*).

The seismic resilience index (*Re*) of the examined tunnel exposed to a certain *IM* level can be derived using the fragility and restoration functions. The latter describes the speed of restoration of functionality for the different *DS*s and the probabilities of occurrence for each *DS*, as discussed in the following sections. Hence, the tunnel functionality at time *t* can be computed as Equation (7) [14,15]:

$$Q(t) = \sum_{j=1}^{4} Q\left[DS_j|t\right] P\left[DS_j|IM\right], \tag{7}$$

where $Q[DS_j \mid t]$ represents the function to restore the functionality of the tunnel at time *t* and damage state *j*, and $P[DS_j \mid IM]$ stands for the conditional probability of a damage state *j* for an event with a given *IM*, which can be calculated by Equations (4) and (5).

2.5. Restoration Function and Time

For the following seismic resilience analysis, because of the lack of a specific restoration function for the studied tunnel, the empirical ones provided by FEMA [27] are used in this work, as presented in Figure 8 in terms of minor, moderate, and extensive damage, derived based on the results from the experts' surveys. It is noted that there is a need for the development of rigorous restoration models that will account more accurately for critical parameters, such as the availability of relevant sources and funds, management approaches in constructions and repairs, and maintenance strategies.

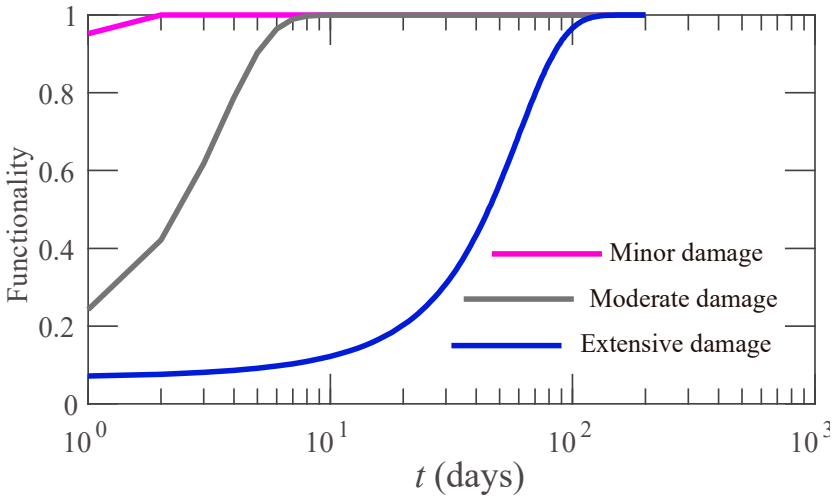

Figure 8. Restoration functions by FEMA [27].

3. Results and Discussion

3.1. Seismic Fragility Assessment

3.1.1. Derivation of Fragility Function Parameters

According to the above considerations, two parameters, i.e., IM_{mi} and β_{tot}, are required to derive the corresponding fragility functions. The value of IM_{mi} for *PGA* or *PGV* concerning the various *DS*s is computed using a regression analysis for the nonlinear numerical results. Particularly in this study, a traditional linear regression analysis is adopted using the natural logarithm of the *DI* and *IM* as the variables. As shown in Figure 9a,b, the different data points (360 in total) stand for the corresponding damage indexes under increasing levels of *PGA*, while the solid blue line indicates the regression fit curve for these Ln(*DI*)–Ln(*IM*) datasets. It is noted that IM_{mi} is computed based on the regression fit equation with the different thresholds of *DS*. β_D is calculated as the dispersion of the different data points with regard to the curve of regression fit [26], and the total lognormal standard deviation β_{tot} is calculated using Equation (2). The detailed fragility function parameters in terms of IM_{mi} and β_{tot} are also presented in Figure 9.

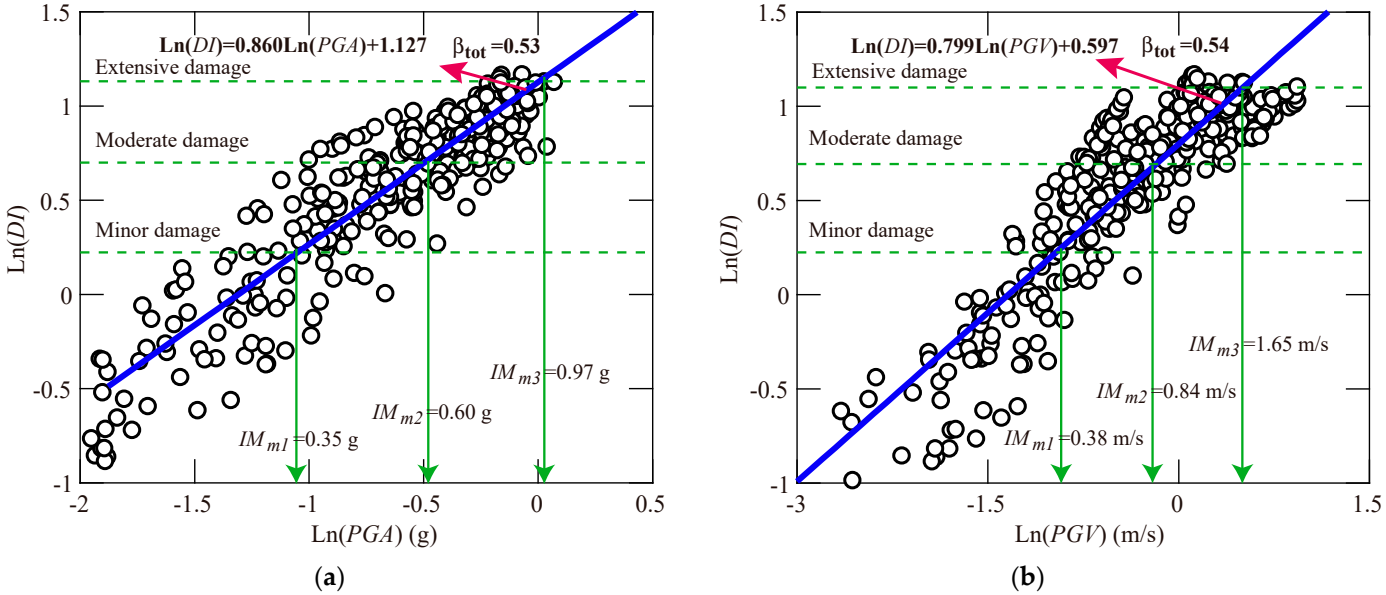

Figure 9. Evolution of the *DI* with (**a**) *PGA* and (**b**) *PGV* at the free-field ground surface.

3.1.2. Development of Fragility Functions

Based on the derived fragility parameters, the corresponding fragility functions can be developed using Equation (1). Figure 10a presents the *PGA*-based fragility functions for the examined tunnel in soft soil. Naturally, the exceedance probability of damage would increase with increasing *PGA*. As the value of *PGA* is lower than 0.3 g, the probability of extensive damage is negligible, which means that the examined shallow tunnel may withstand this level of earthquake intensity well, practically with no damage. The minor and moderate damage probabilities are 15% and 2%, respectively. When *PGA* equals 0.4 g, the exceedance probabilities for minor, moderate, and extensive damage will increase to 60%, 22%, and 5%, respectively. In comparison, as the value of *PGA* increases to near 1.0 g, there is a 97% probability that the tunnel will be exposed to minor damage. The relevant possibilities for moderate or extensive damage are 83% and 52%. The latter observations highlight the significant importance of sufficient seismic designs for shield tunnels in similar sites. Similar conclusions can also be obtained for the fragility functions developed in terms of *PGV* at the ground surface.

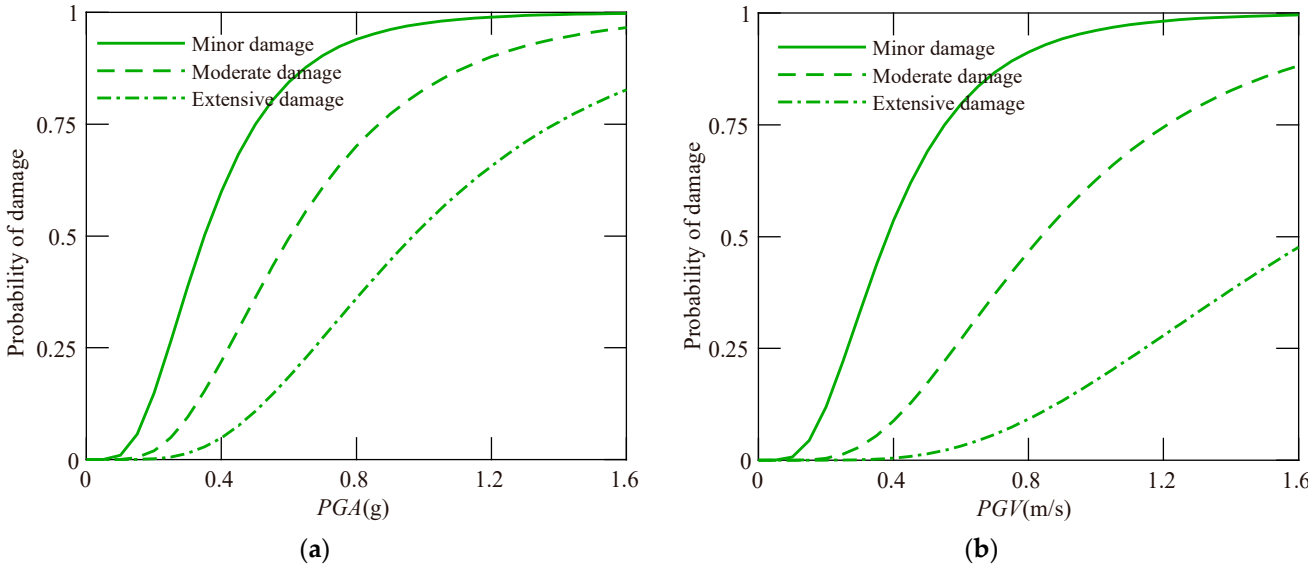

Figure 10. Developed fragility functions by (**a**) *PGA* and (**b**) *PGV* at the ground surface.

3.2. Seismic Loss Assessment

Figure 11a,b provide the calculated direct seismic loss curves for the examined tunnel in terms of *PGA* and *PGV*, respectively. The fundamental trends of seismic loss curves are in line with the corresponding fragility functions. Using the derived loss curves, the repair cost of each tunnel ring (per meter) could be calculated for various seismic levels. For example, suppose a metro line is exposed to an earthquake intensity of *PGA* = 0.5 g. In that case, the total repair cost for the examined tunnel could easily be found to be 180,000 RMB from Figure 11a, indicating that rather essential repairs would be required for each tunnel segment. Similar conclusions may be drawn by examining Figure 11b, where the *IM* is given in terms of *PGV*. In this way, the proposed direct seismic loss curves can be employed in the quantitative risk assessment of the metro tunnel network subjected to seismic loading.

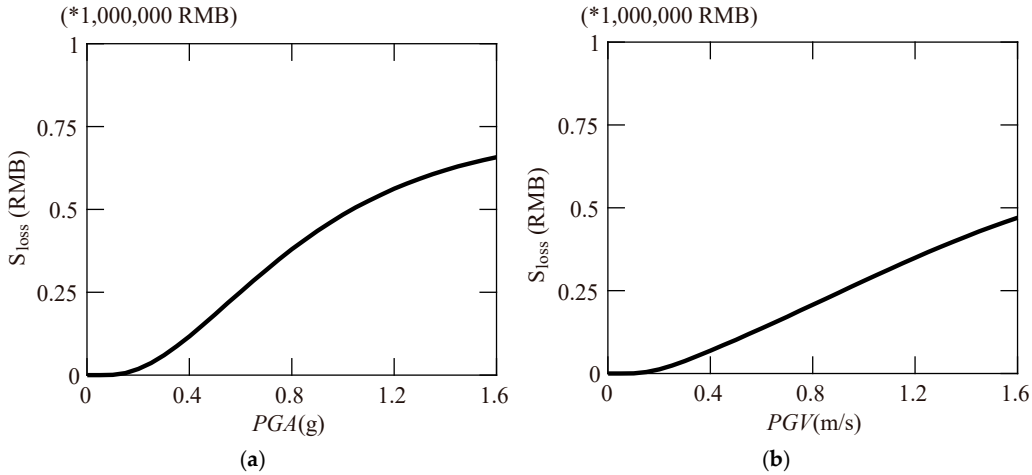

Figure 11. Direct seismic loss of the examined tunnel in terms of (**a**) *PGA* and (**b**) *PGV* at the free-field ground surface.

3.3. Seismic Resilience Assessment

3.3.1. Tunnel Functionality Assessment

According to Equation (3), the tunnel functionality $Q(t)$ at time t is calculated by the developed fragility functions and functionality restoration functions [27]. Figure 12a,b

present the influences of five different values of *PGA* (0.2, 0.4, 0.6, 0.8, and 1.0 g) and five different values of *PGV* (0.2, 0.4, 0.6, 0.8, and 1.0 m/s) on the development of tunnel functionality, $Q(t)$. As expected, the damage induced by a lower seismic intensity (*PGA* or *PGV*) seems to be more easily recovered from, indicating a higher resilience index (*Re*) with lower *PGA* and *PGV* for the studied tunnel.

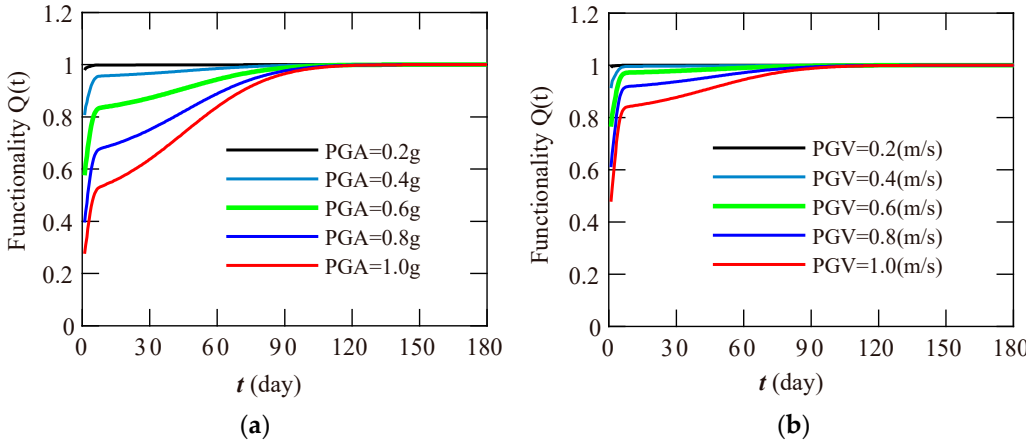

Figure 12. Functionality recovery function of the examined tunnel in terms of (**a**) *PGA* and (**b**) *PGV* at free-field ground surface.

3.3.2. Development of the Resilience Index

Figure 13a,b show the resilience index (*Re*)'s evolution for the studied tunnel under the different *PGA* and *PGV* values, respectively. Naturally, it is clearly demonstrated that the seismic resilience index of tunnels decreases gradually when the *PGA* or *PGV* increases. More specifically, as the *PGA* is ranged between 0.0 g and 1.0 g, the resilience of tunnels is found to remain at a level between 0.87 and 0.99. It is more significant in the case of *PGV*, for it is indicated that the resilience of tunnels maintains a high level between 0.95 and 0.99 when the *PGV* is ranged between 0.0 m/s and 1.0 m/s. From the above analysis, it is concluded that the examined tunnel is generally good in terms of seismic resilience. Nevertheless, the critical roles of adequate seismic design of the tunnel structure and rapid recovery measures at the post-earthquake event in case of severe seismic intensities have been demonstrated.

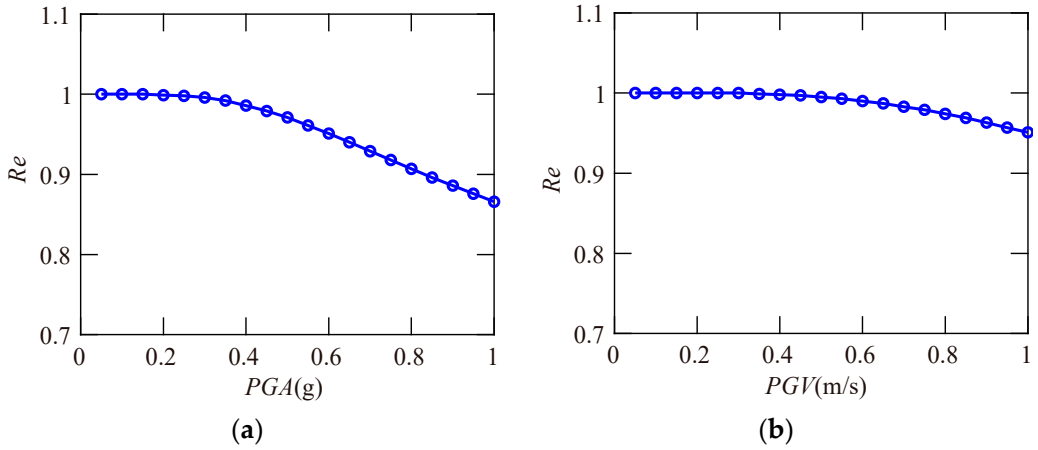

Figure 13. Resilience index *Re* of the examined tunnel in terms of (**a**) *PGA* and (**b**) *PGV* at the free-field ground surface.

3.3.3. Effects of Different Fragility Functions on Tunnel Resilience

A crucial issue for the resilience evaluation of tunnels is the selection of appropriate fragility functions [29–31]. Indeed, the use of different fragility functions may lead to distinct probabilities of being in a particular damage state and hence may affect the resilience index estimated for an examined tunnel. To highlight this issue, an example is provided to study the effects of different fragility functions on tunnel resilience. More specifically, the analytical fragility functions provided through this study, Argyroudis and Pitilakis [26] and Argyroudis et al. [32], as well as the empirical fragility functions provided by ALA [33], are used to compute the resilience index *Re* for the examined case.

Figure 14 illustrates the variation of the resilience index (*Re*) with increasing levels of the seismic intensity measure (*PGA*), as computed for the examined soil–tunnel configurations by employing different fragility functions. Evidently, a significant scatter is observed by comparing the *Re* computed for different levels of seismic *IM* when using different fragility functions. In particular, for a specific level of seismic intensity, the use of the empirical fragility functions provided by ALA [33] leads to the highest values of *Re* compared to the values computed when using the analytical fragility functions. On the contrary, the lowest *Re* values are obtained when using the analytical fragility functions presented by Argyroudis and Pitilakis [26]. These observations are attributed to different modelling approaches and assumptions utilized to generate the selected fragility functions. The empirical fragility functions provided by ALA [33] are derived using reports of actual damage of tunnels from past earthquakes as well as expert judgements. The numerical fragility functions provided by Argyroudis and Pitilakis [26] are developed through a couple of numerical analyses of soil–tunnel configurations, with the seismic loading being simulated by employing a quasi-static method. The numerical fragility functions proposed by Argyroudis et al. [32] are generated according to the results of a set of non-linear numerical simulations considering soil-structure interaction phenomena in a more rigorous fashion. Finally, the analytical fragility functions provided by this study are proposed by employing the results of non-linear dynamic analyses of the soil–tunnel configuration, considering the effects of local soil conditions of Shanghai city. Differences in the assumptions made regarding the geometrical properties of the soil–tunnel configuration, the implemented soil constitutive models, and the considered ground motion characteristics may have also affected the computed fragilities of the examined tunnels, hence affecting the computed resilience index of the examined configurations. The above discrepancies reveal the need for further investigation of the seismic fragility and resilience of tunnels.

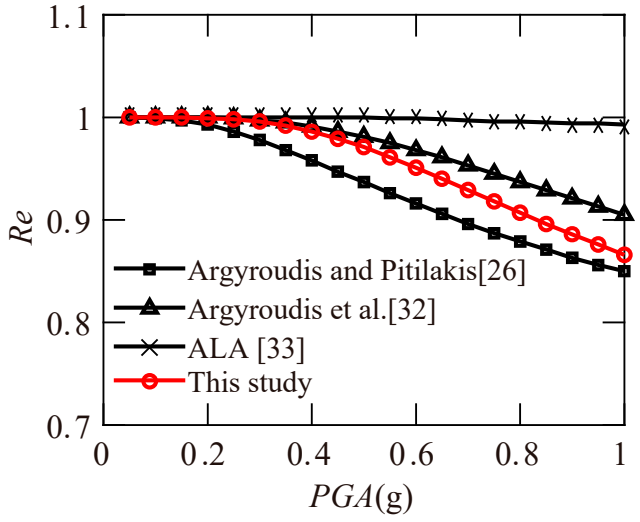

Figure 14. Resilience index (*Re*) of the examined tunnel using different empirical and numerical fragility functions.

4. Conclusions

The present work aimed to assess the resilience of shallow circular tunnels in soft soil areas exposed to earthquakes based on derived fragility functions. The following conclusions can be obtained through the above analyses:

(1) The exceedance probabilities, direct seismic losses, and seismic resilience indexes of the examined tunnels are thoroughly evaluated with various earthquake intensity measures (*IM*s), i.e., *PGA* or *PGV*, which is beneficial for the post-earthquake strategic recovery planning.
(2) It is revealed that an increase in the earthquake intensity measure (*IM*), i.e., *PGA* or *PGV*, for different damage states will lead to a significant increase in recovery time and direct seismic loss, which will also affect the tunnels' functionality.
(3) The effects of different fragility functions on tunnel resilience are identified and the importance of selection of appropriate fragility functions in resilience assessments of tunnels is highlighted accordingly.
(4) The evolution of tunnel seismic resilience demonstrates the important role of adequate seismic design of tunnel structures and rapid recovery measures at the post-earthquake event for the various seismic intensities.
(5) The results of this study also highlight the requirements of seismic resilience assessment for better evaluation of seismic risk, earthquake emergency management, and recovery strategy planning for tunnel structures.

The proposed seismic resilience evaluation framework can also be extended to other types of underground structures by using more realistic restoration functions and further considering the effects of aging phenomenon [34] and potential multiple hazards [35]. Moreover, it is noted that the present work only considers horizontal earthquakes in the seismic analysis. Further studies could also consider the effect of the vertical components of earthquakes so as to obtain more accurate seismic fragility and resilience assessment results.

Funding: This research was funded by the National Natural Science Foundation of China (52108381, 52090082, 51978517), the Shanghai Science and Technology Committee Program (21DZ120060, 20DZ1201404), the National Key Research and Development Program of China (2021YFF0502200), and the China Postdoctoral Science Foundation (2021M702491).

Institutional Review Board Statement: Not applicable.

Informed Consent Statement: Not applicable.

Data Availability Statement: All data generated or analyzed during this study are included in this published article.

Acknowledgments: The author would like to thank the editors, reviewers, Tianyi Wang, and Dongmei Zhang for their helpful and constructive comments that greatly contributed to improving the quality of the paper.

Conflicts of Interest: The author declares no conflict of interest.

References

1. Wang, W.L.; Wang, T.T.; Su, J.J.; Lin, C.H.; Seng, C.R.; Huang, T.H. Assessment of damage in mountain tunnels due to the Taiwan Chi-Chi earthquake. *Tunn. Undergr. Space Technol.* **2001**, *16*, 133–150. [CrossRef]
2. Li, T. Damage to mountain tunnels related to the Wenchuan earthquake and some suggestions for aseismic tunnel construction. *Bull. Eng. Geol. Environ.* **2012**, *71*, 297–308. [CrossRef]
3. Hashash, Y.M.; Hook, J.J.; Schmidt, B.; John, I.; Yao, C. Seismic design and analysis of underground structures. *Tunn. Undergr. Space Technol.* **2001**, *16*, 247–293. [CrossRef]
4. Bruneau, M.; Chang, S.E.; Eguchi, R.T.; Lee, G.C.; O'Rourke, T.D.; Reinhorn, A.M.; Shinozuka, M.; Tierney, K.; Wallace, W.A.; Von Winterfeldt, D. A framework to quantitatively assess and enhance the seismic resilience of communities. *Earthq. Spectra* **2003**, *19*, 733–752. [CrossRef]
5. Cimellaro, G.P.; Reinhorn, A.M.; Bruneau, M. Framework for analytical quantification of disaster resilience. *Eng. Struct.* **2020**, *32*, 3639–3649. [CrossRef]

6. Biondini, F.; Camnasio, E.; Titi, A. Seismic resilience of concrete structures under corrosion. *Earthq. Eng. Struct. Dyn.* **2015**, *44*, 2445–2466. [CrossRef]
7. Asadi, E.; Salman, A.M.; Li, Y.; Yu, X. Localized health monitoring for seismic resilience quantification and safety evaluation of smart structures. *Struct. Saf.* **2021**, *93*, 102127. [CrossRef]
8. Alipour, A.; Shafei, B. Seismic resilience of transportation networks with deteriorating components. *J. Struct. Eng.* **2016**, *142*, C4015015. [CrossRef]
9. Sun, W.; Bocchini, P.; Davison, B.D. Resilience metrics and measurement methods for transportation infrastructure: The state of the art. *Sustain. Resilient Infrastruct.* **2020**, *5*, 168–199. [CrossRef]
10. Argyroudis, S.A. Resilience metrics for transport networks: A review and practical examples for bridges. *Proc. Inst. Civ. Eng. Bridge Eng.* **2021**. [CrossRef]
11. Bruneau, M.; Reinhorn, A. Exploring the concept of seismic resilience for acute care facilities. *Earthq. Spectra* **2007**, *23*, 41–62. [CrossRef]
12. Shang, Q.; Wang, T.; Li, J. A quantitative framework to evaluate the seismic resilience of hospital systems. *J. Earthq. Eng.* **2020**, 1–25. [CrossRef]
13. Samadian, D.; Ghafory-Ashtiany, M.; Naderpour, H.; Eghbali, M. Seismic resilience evaluation based on vulnerability curves for existing and retrofitted typical RC school buildings. *Soil Dyn. Earthq. Eng.* **2019**, *127*, 105844. [CrossRef]
14. Gonzalez, C.; Niño, M.; Jaimes, M.A. Event-based assessment of seismic resilience in Mexican school buildings. *Bull. Earthq. Eng.* **2020**, *18*, 6313–6336. [CrossRef]
15. Anwar, G.A.; Dong, Y. Seismic resilience of retrofitted RC buildings. *Earthq. Eng. Eng. Vib.* **2020**, *19*, 561–571. [CrossRef]
16. Tirca, L.; Serban, O.; Lin, L.; Wang, M.; Lin, N. Improving the seismic resilience of existing braced-frame office buildings. *J. Struct. Eng.* **2016**, *142*, C4015003. [CrossRef]
17. Decò, A.; Bocchini, P.; Frangopol, D.M. A probabilistic approach for the prediction of seismic resilience of bridges. *Earthq. Eng. Struct. Dyn.* **2013**, *42*, 1469–1487. [CrossRef]
18. Capacci, L.; Biondini, F. Probabilistic life-cycle seismic resilience assessment of aging bridge networks considering infrastructure upgrading. *Struct. Infrastruct. Eng.* **2020**, *16*, 659–675. [CrossRef]
19. Huang, Z.K.; Argyroudis, S.A.; Pitilakis, K.; Zhang, D.M.; Tsinidis, G. Fragility assessment of tunnels in soft soils using artificial neural networks. *Undergr. Space* **2022**, *7*, 242–253. [CrossRef]
20. Tran, T.T.; Cao, A.T.; Kim, D.; Chang, S. Seismic vulnerability of cabinet facility with tuned mass dampers subjected to high-and low-frequency earthquakes. *Appl. Sci.* **2020**, *2020. 10*, 4850. [CrossRef]
21. Nguyen, V.T.; Ahn, J.H.; Haldar, A.; Huh, J. Fragility-based seismic performance assessment of modular underground arch bridges. *Structures* **2022**, *39*, 1218–1230. [CrossRef]
22. Huang, H.W.; Zhang, D.M. Resilience analysis of shield tunnel lining under extreme surcharge: Characterization and field application. *Tunn. Undergr. Space Technol.* **2016**, *51*, 301–312. [CrossRef]
23. Huang, Z.K.; Zhang, D.M.; Zhou, Y.T. Resilience Assessment Framework for Tunnels Exposed to Earthquake Loading. In Proceedings of the 4th International Conference on Performance-Based Design in Earthquake Geotechnical Engineering (PBD-IV), Beijing, China, 15–17 July 2022; in press.
24. CEN (European Committee for Standardization). *Eurocode 8: Design of Structures for Earthquake Resistance*; CEN: Brussels, Belgium, 2004.
25. Lysmer, J.; Kuhlemeyer, R.L. Finite dynamic model for infinite media. *J. Eng. Mech. Div.* **1969**, *95*, 859–878. [CrossRef]
26. Argyroudis, S.A.; Pitilakis, K.D. Seismic fragility curves of shallow tunnels in alluvial deposits. *Soil Dyn. Earthq. Eng.* **2012**, *35*, 1–12. [CrossRef]
27. FEMA (Federal Emergency Management Agency). *Hazus 4.2 SP3: Hazus Earthquake Model Technical Manual*; FEMA: Washington, DC, USA, 2020.
28. Werner, S.D.; Taylor, C.E.; Cho, S.; Lavoie, J.P.; Huyck, C.K.; Eitzel, C.; Chung, H.; Eguchi, R.T. *Redars 2 Methodology and Software for Seismic Risk Analysis of Highway Systems*; Special Report MCEER-060SP08; MCEER (Multidisciplinary Center Earthquake Engineering Research): New York, NY, USA, 2006.
29. Karamlou, A.; Bocchini, P. Computation of bridge seismic fragility by large-scale simulation for probabilistic resilience analysis. *Earthq. Eng. Struct. Dyn.* **2015**, *44*, 1959–1978. [CrossRef]
30. Pang, Y.; Wang, X. Cloud-IDA-MSA conversion of fragility curves for efficient and high-fidelity resilience assessment. *J. Struct. Eng.* **2021**, *147*, 04021049. [CrossRef]
31. Gidaris, I.; Padgett, J.E.; Barbosa, A.R.; Chen, S.; Cox, D.; Webb, B.; Cerato, A. Multiple-hazard fragility and restoration models of highway bridges for regional risk and resilience assessment in the United States: State-of-the-art review. *J. Struct. Eng.* **2017**, *143*, 04016188. [CrossRef]
32. Argyroudis, S.; Tsinidis, G.; Gatti, F.; Pitilakis, K. Effects of SSI and lining corrosion on the seismic vulnerability of shallow circular tunnels. *Soil Dyn. Earthq. Eng.* **2017**, *98*, 244–256. [CrossRef]
33. ALA (American Society of Civil Engineers-FEMA). *Seismic Fragility Formulations for Water Systems: Part 1-Guideline*; ALA: Washington, DC, USA, 2001.

34. Huang, Z.K.; Argyroudis, S.; Zhang, D.M.; Pitilakis, K.; Huang, H.W.; Zhang, D.M. Forthcoming. Time-dependent fragility functions for circular tunnels in soft soils. *ASCE-ASME J. Risk Uncertain. Eng. Syst. Part A Civ. Eng.* **2022**. [CrossRef]
35. Huang, Z.K.; Pitilakis, K.; Argyroudis, S.; Tsinidis, G.; Zhang, D.M. Selection of optimal intensity measures for fragility assessment of circular tunnels in soft soil deposits. *Soil Dyn. Earthq. Eng.* **2021**, *145*, 106724. [CrossRef]